Advancing Surgical Vision with Fluorescence Imaging

Maximilian Koch[1,2] and Vasilis Ntziachristos[1,2]

[1]Helmholtz Zentrum München, German Research Center for Environmental Health, Institute for Biological and Medical Imaging, 85764 Neuherberg, Germany;
email: maximilian.koch@helmholtz-muenchen.de

[2]Munich School of Bioengineering, Translational Oncology Center (TRANSLATUM), Technische Universität München (TUM), 81675 Munich, Germany;
email: v.ntziachristos@tum.de

Annu. Rev. Med. 2016. 67:153–64

The *Annual Review of Medicine* is online at med.annualreviews.org

This article's doi:
10.1146/annurev-med-051914-022043

Keywords

intraoperative imaging, molecular imaging, fluorescence agents, targeted fluorescence imaging, sentinel lymph node mapping

Abstract

Surgical success depends on the accuracy with which disease and vital tissue can be intraoperatively detected. However, the dominant visualization approach, i.e., human vision, does not see under the tissue surface and operates on low contrast between sites of disease, such as cancer, and the surrounding tissue. Intraoperative fluorescence imaging is emerging as a highly effective method to improve surgical vision and offers the potential to be intergrated seamlessly into the normal workflow of the operating room without causing disruption or undue delay. We review and compare two critical fluorescence imaging directions: one that uses nonspecific fluorescence dyes, addressing tissue perfusion and viability, and one that uses targeted agents, interrogating pathophysiological features of disease. These two approaches present detection sensitivity challenges that may differ by orders of magnitude and require different detection strategies. Nevertheless, fluorescence imaging provides the surgeon with previously unavailable real-time feedback that improves surgical precision and can become essential for interventional decision-making.

INTRODUCTION

Surgery plays a major role in the therapy of many diseases, including cancer and cardiovascular and neurological disorders. Our conventional view of the operating room today contains a paradox. On the one hand, advanced technology surrounds the surgeon, from elaborate vital-sign monitoring to the tools of laparoscopic and robotic surgery. On the other hand, intraoperative guidance is primarily based on human vision and tactile information, a scheme unaltered since the beginning of medicine. Radiological techniques such as X-ray imaging and magnetic resonance imaging are employed for preoperative planning, but their ability to guide the surgeon during the procedure is limited (1, 2); the size of the equipment is not appropriate for the confined conditions of the operating room and the proximity required between a surgical team and the patient. Tomography scanners come at a cost that limits general use in the operating room, and they do not offer the resolution and contrast required for intraoperative guidance. X-ray imaging, for example, employed in a C-arm configuration, does not give sufficient contrast or resolution for visualizing infiltrating cancer borders or detecting lymph node metastasis. Portable imaging systems have been successfully tried but also have limitations. For example, because gamma cameras have low resolution and require the administration of radioactive tracers, they are used in the operating room primarily for identifying lymph nodes in some operations for cancer (3).

Despite imaging advances over the past decades, disease detection during surgery today is still based on direct eyesight visualization or evaluation of white light images through a microscope or on a computer monitor. Tactile information is available in open surgery, but the gradual shift to minimally invasive procedures such as laparoscopy and robotic surgery leaves the surgeon with only visual ability, further limiting the information available for intraoperative decision making. The prevalent technologies associated with surgical and endoscopic visualization relate to (*a*) high-definition optical systems, i.e., white light imaging with high-resolution analysis [up to 1,280 × 1,024 pixels (4)] or (*b*) stereoscopic information, which offers the surgeon high-resolution three-dimensional image perception (5).

Human vision, either through direct eyesight or through an optical system, comes with important limitations in detecting disease and differentiating it from healthy tissue and tissue structures. Human vision does not have adequate sensitivity to detect cells, molecules, or processes associated with physiological and biochemical alterations in cancer, stroke, or tissue perfusion. Moreover, optical imaging and human vision cannot visualize under the tissue surface. Therefore disease infiltration or subsurface tissue morphology and structures, including lymph nodes, major vessels, and nerves, cannot be detected. Likewise, functional tissue information, including tissue perfusion and oxygenation, is a critical metric in several surgical procedures including vascular surgery, intestinal anastomoses, and plastic surgery but is not available to visual inspection. Modern surgery is therefore often confronted with limitations in identifying disease, vital tissue structures, or tissue function, leading to surgical uncertainty, complicating decision making, and prolonging the surgical procedure.

The injection of fluorescent substances, such as fluorescein/fluorescein isothiocyanate (FITC) or indocyanine green (ICG), to aid surgical visualization is a 70-year-old concept (6, 7). Fluorescence imaging offers potent advantages over human vision, e.g., imaging of subsurface structures through depths of several millimeters to centimeters, especially when using near-infrared dyes. Fluorescence modalities employ nonionizing radiation and stable fluorochromes that do not impose time constraints, as decaying radioisotopes typically do. The method can seamlessly integrate into the normal flow of activity in the operating room, thanks to small size and cost-effectiveness, and can be combined with optical endoscopes or white light cameras and microscopes in hybrid systems. Despite these promising characteristics and its 70-year history, intraoperative imaging

with fluorescence has not become standard of care in surgery but remains investigational. We explain herein potential uses of fluorescence imaging in the operating room and outline the compelling reasons for the technology to become a mainstream procedure within the next decade. We first discuss applications using fluorescent dyes that distribute in the vascular system and then turn to fluorescence agents that have specificity for particular features of disease and are especially well suited for oncological surgery. Use of targeted versus nontargeted fluorescent moieties define different detection requirements, summarized herein. Finally, we discuss pitfalls and challenges that will need to be overcome to ensure successful propagation in clinical practice.

NONSPECIFIC FLUORESCENT DYES

Fluorescent dyes that distribute in the vascular system are useful for revealing morphological and physiological tissue parameters in intraoperative applications. ICG has been used since the 1950s to enable studies of hepatic clearance (8), cardiac output (9), and retinal vasculature (10). Its off-label use for tissue perfusion studies or lymph node mapping in various surgical procedures has been reported (11, 12).

Tissue Perfusion and Viability

Various operations require real-time assessment of tissue function and accurate characterization of viable versus nonperfused, nonviable tissue. However, human vision cannot accurately measure tissue oxygenation or perfusion. ICG video-angiography observes tissue fluorescence enhancement over time, following the intravascular administration of ICG. Because ICG is primarily contained within the vascular system, the technique allows vascular flow to be visualized in real time and has been employed to assess peripheral tissue perfusion in organ transplantation (13) and plastic surgery (14). In cardiac surgery, ICG can help evaluate graft patency (15). Likewise, the effects of venous sacrifice during neurosurgery could be assessed by clipping the vessel and assessing collateral circulation using ICG video-angiogram (16).

ICG has also been employed to monitor anastomotic procedures. Poor tissue perfusion/oxygenation can lead to anastomotic dehiscence at rates of up to 15% (17), with corresponding risks of mortality, especially in the older population, and considerable morbidity, i.e., sepsis, reoperation, resection of the anastomosis, creation of a definitive colostomy, prolonged hospital stay, and Intensive Care Unit admission. ICG visualization of colorectal anastomotic perfusion has been performed in rectal surgery (18). Tissue perfusion is likewise a vital parameter in plastic surgery (19). In mastectomy or oncoplastic reconstructive surgery associated with breast cancer, muscle flaps are transposed from other parts of the body to the breast area. These flaps may become poorly oxygenated or perfused, leading to ischemia and potentially necrosis (20). Other plastic surgery–related ICG imaging interventions are documented for preoperative planning and intra- or postoperative assessment, including flap reconstruction, lymphedema, and detection of skin perforators (21, 22).

Lymph Node Mapping

In surgical oncology, sentinel lymph node (SLN) resection and evaluation are commonly performed. The excised SLN can be analyzed immediately by cryo-sectioning (23) or examined later in more detail by the pathologist (24). Identification of metastatic cancer in lymph nodes provides critical staging information for treatment planning. The intraoperative localization of lymph nodes is, however, complicated because lymph nodes are often embedded deep within adipose tissue and

not accessible to visual inspection. Mapping of SLNs has been performed by the intratumoral injection of visible dyes such as methylene blue or radioisotope tracers detected by gamma sensors (25). ICG imaging avoids the use of radioactivity and can sense lymph nodes deeper than methylene blue (11) because ICG emits fluorescence light in the near-infrared range. This concept has been clinically demonstrated in breast cancer (26–28), skin cancer (29), squamous cell carcinoma (30), vulvar cancer (31), cervical cancer (32), endometrial cancer (33), and lung cancer (34). In addition to the SLN, fluorescence imaging can identify many more nodes, since all tumor-draining nodes will be fluorescently enhanced following intratumoral ICG administration (35). Assuming that the enhancement of nodes is followed over time, information on the first draining node can be obtained.

ICG-based SNL mapping is seen as a balanced strategy between complete lymphadenectomy, which is time consuming and risks side effects, and absence of nodal evaluation, which may necessitate additional radiation or systemic therapy (36). Fluorescence guidance increases precision (**Figure 1**) in reliably identifying the SNL and other nodes and minimizing damage to surrounding healthy tissue. Administered during the primary procedure aiming at tumor removal, the method does not introduce significant additional costs and could accelerate the procedure by faster localization of the nodes of interest (37). The use of targeted agents may further enhance identification of locoregional cancer metastasis, as discussed below.

An important further aspect of fluorescence imaging is that it helps compensate for the loss of tactile information in minimally invasive procedures, including robotic surgery. For this reason, ICG has been studied enhancing robotic surgery and has demonstrated potential in several applications (38), including SLN visualization and lymph node mapping (39), investigation of astomotic perfusion (38, 40), and the visualization of the biliary tree anatomy in robot-assisted cholecystectomy (41).

SPECIFIC AGENTS

Dyes such as ICG can preferentially distribute to tumors through the enhanced permeability retention effect but have not so far demonstrated consistent specificity for outlining tumors and tumor margins. Attention has instead shifted to the use of fluorescence agents to identify molecular-based biomarkers that are upregulated in cancer (**Figure 2**). Although many biomarkers are typically reported to play an important role in different cancers, only a limited number of these markers are suitable for tumor targeting, and prioritization is necessary to ensure optimal imaging signals (42). Critical criteria for selecting fluorescence probes include a broad upregulation profile in many cancers, favorable biodistribution characteristics, available amplification strategies (e.g., the agent is activatable or is internalized in cells), and prior experience (e.g., molecules already known as pharmaceuticals can be labeled) (43).

Primary Cancer

In oncological surgery, complete removal of the tumor improves prognosis and decreases recurrence of disease for many cancer types (44–46). However, in the absence of real-time feedback during surgery, only postoperative inspection of tissue specimen with histopathology can identify complete resection or the presence of positive margins indicative of an incomplete excision. Typically it is several hours to days after surgery before the specimen is analyzed and the presence of positive margins is confirmed.

Secondary procedures may be necessary due to incomplete first surgery, which adds to the patient's stress and healthcare cost. Rates of repeat surgery vary widely by doctor and institution,

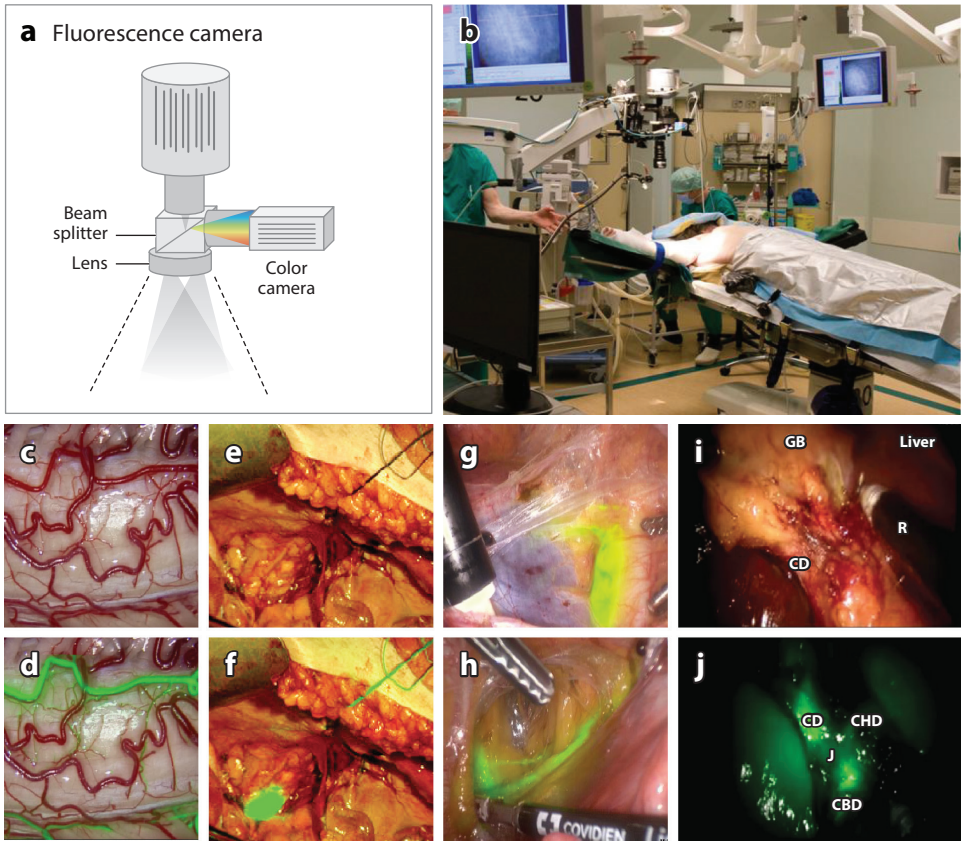

Figure 1

Indocyanine green (ICG)-enhanced interventional imaging. (*a*) Typical intraoperative fluorescence imaging system using simultaneous image collection from a fluorescence and white light (color) camera visualizing the same field of view through a common optical system (beam splitter and lens). Instead of a lens, an endoscope system could be connected (as used in 31, 32, 50). (*b*) Photograph of a camera in the operating room. The camera is placed above the patient; white light, fluorescence, and overlay images can be projected on monitors in the operating room. Typically the camera is wrapped in sterile drapes (not shown here). From Reference 50 with permission. (*c*) Color reflection image of the spinal cord and (*d*) ICG-based video-angiography: The fluorescence signal was overlaid on the color reflection image. The image was rendered by alpha-blending the fluorescence values after spatial anatomical landmark registration from images published in Reference 72. ICG-angiography visualized the microvascular flow and anatomical orientation, necessary to ensure safe and precise resection of spinal intramedullary tumors. The image shows an early stage shortly after ICG injection highlighting the posterior spinal arteries on both sides. (*e*) White light reflection (*f*) overlaid with a fluorescence image revealing a lymph node in early-stage cervical cancer surgery. The lymph node cannot be identified by human vision on the white light image as it is located under the tissue surface. Images *e* and *f* from Reference 32 with permission. (*g*) Endoscopic sentinel lymph node (SLN) mapping in the right external iliac region after cervical ICG injection in a woman with endometrial cancer and (*h*) endoscopic cervical lymph node mapping in the left obturator region likewise reveal a lymph node hidden under the tissue surface and not visible to the eye (36). (*i*) Color reflection image and (*j*) fluorescence pseudo-color image of intraoperative fluorescent cholangiography during robotic single-site cholecystectomy. The fluorescence image contributed to the identification of the extrahepatic biliary anatomy, necessary to minimize the risk of biliary injury. Abbreviations: CBD, common bile duct; CD, cystic duct; CHD, common hepatic duct; GB, gallbladder; J, junction between cystic duct and common hepatic duct; R, robotic instrument. Images *i* and *j* from Reference 73 with permission.

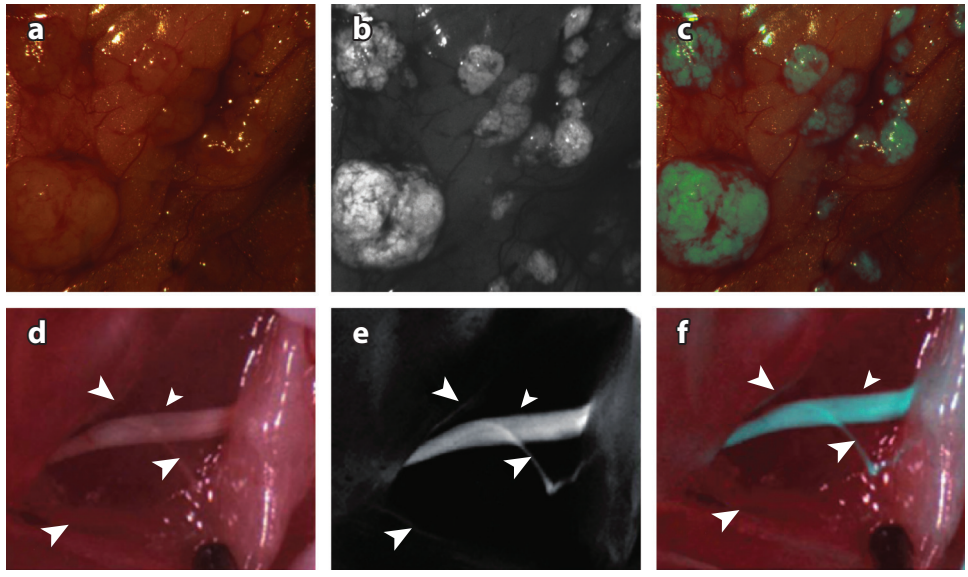

Figure 2

During palliative surgery in an ovarian cancer patient, the same view is shown as (*a*) a white light image, (*b*) a fluorescence image, and (*c*) a white light image with fluorescence overlay (in pseudogreen) from fluorescence imaging of a folate receptor-α targeting agent (50). The study demonstrated that tumor foci not visible to the human eye could be visualized in fluorescence mode. (*d*) White light, (*e*) fluorescence, and (*f*) white light images with fluorescence overlay (in pseudoblue) of an in vivo nerve-targeting fluorescence peptide in mice (64) show the sciatic nerve branching within muscle planes. The bigger branch of the nerve is clearly visible (*small arrowheads*), whereas the smaller branches are difficult to discriminate (*large arrowheads*). The fluorescence and overlay images depict signal from large and small nerves. Images *d*, *e*, and *f* from Reference 64 with permission.

from 0% to 70% (47), and studies have reported up to 40% of intended curative resections containing microscopic evidence of residual tumor (44, 48). Similar limitations are also reported in endoscopic procedures, such as laparoscopic colorectal surgery (48, 49). The uncertainty about resection margins directs excision of large volumes of healthy tissue around the tumor, leading to irreversible tissue damage (e.g., in vital structures such as nerves) and postoperative complications. Real-time intraoperative feedback in this case can improve decision making, management, and the planning of follow-up treatment (radiotherapy, chemotherapy).

Different agents and targets have been considered. An agent targeting folate receptor-α conjugated to FITC was systemically injected prior to laparotomy and yielded visualizations more than five times more accurate than white light contrast (50). Topical administration of a targeted fluorescence heptapeptide was evaluated during endoscopic intervention for detection of colonic dysplasia using confocal endomicroscopy (51). A tumor necrosis factor (TNF)-targeting antibody has been employed to visualize $mTNF^+$ immune cells and correlated the mean cell number to the short-term Crohn's disease response rates (52). High-grade Barrett's neoplasia was also visualized using a FITC-labled peptide (53).

The potential of utilizing drugs labeled with fluorescence dyes has been recently discussed (54). The extension of approved therapeutics to intraoperative imaging is being evaluated clinically (see ClinicalTrials.gov NCT01508572, NCT02113202, NCT01972373, NCT02129933, NCT01987375, NCT02415881) using labeled bevacizumab, cetuximab, or panitumumab, all

conjugated to IRDye 800CW (LI-COR Biosciences, Lincoln, NE, USA). Cetuximab-800CW imaging in head and neck squamous cell carcinoma patients differentiated tumor from normal tissue during resection with an average tumor-to-background ratio of 5.2, with fluorescence levels positively correlated with epidermal growth factor receptor (EGFR) levels (55).

Induced cancer fluorescence has also been exploited for intraoperative imaging. Oral administration of 5-aminolevulinic acid (5-ALA) has been shown to induce protoporphyrin IX (PpIX) in high-grade glioma (56). 5-ALA-induced PpIX fluorescence detection was shown to enhance the rate of complete tumor resection and improve progression-free survival in a randomized controlled multicenter phase III trial (57), and to detect the majority of cerebral metastases (58). In addition, induced PpIX has been employed in detecting lymph node metastasis in gastric (59) and colorectal (60) cancer patients.

Metastasis and Staging

Real-time visual feedback from targeted fluorescence agents could enable more accurate determination of locoregional invasion and lymph node metastases, improving cancer staging, treatment selection, and outcome. ICG-based fluorescence can improve guidance to the SNL and other lymph nodes, but lymph node excision for histopathological examination is nevertheless a mutilating process that damages the lymphatic system and may lead to edema and infection. Additionally, histopathological examination of nodes may fail to identify how many nodes are affected, even in case of a positive SNL. Identification of positive lymph nodes without dissection, i.e., the clinical assessment of cancer spread to lymph nodes, is important for determining prognosis, identifying affected lymph nodes for removal, and minimizing side effects. Positron emission tomography (PET) is employed for lymph node staging (61, 62), but the radiological view and the intraoperative view differ significantly, preventing accurate navigation during surgery.

The use of targeted agents can play a critical role in detecting cancer metastasis in nodes, enhancing surgical guidance and pathological staging (37). A promising future strategy for lymph node imaging could be based on the spectral capability of fluorescence imaging. A two-step approach for mapping and subsequent nondestructive classification of SLNs is promising but depends on the cancer-targeting success of the agent employed. In particular, the combination of a nontargeted tumor-injected fluorescence label with an emission spectrum that can spectrally separate it from a targeted fluorescence agent can be used for navigating to lymph nodes and assessing metastatic involvement without excision. The concurrent injection of EGFR-targeted and nontargeted tracer directly into the tumor in an athymic mouse model of metastatic human breast cancer has been tested for mapping and classifying SLNs by accurately quantifying tumor burden, with reported sensitivity of 200 cells (63).

In summary, a method for identifying lymph nodes in the operating room and assessing their cancer status could lead to the in vivo interrogation of a larger number of nodes, simplify surgical procedures, and produce an integrated surgical decision-making platform.

Other Tissues

Targeted agents can be also useful in avoiding damage to sensory or sacral nerves or lymphatics (64), which decreases postoperative quality of life. Nerve targeting has been visualized using a small-molecule distyrylbenzene dye and red-shifted derivatives, crossing the blood-nerve and blood-brain barriers in mice, rats, and pigs (65). Improvements in aqueous solubility and reduced lipophilicity of distyrylbenzene dyes have been demonstrated (66). Alternative targeting molecules, including oxazine dyes and rhodamine, have also been considered (67). Such agents can be combined with tumor-targeting agents, using fluorochromes emitting at different spectral regions along with dual-fluorescence detection cameras.

DETECTION OF TARGETED VERSUS NONTARGETED DYES

The concentrations achieved when using nontargeted dyes (e.g., ICG) to outline the vascular system vary significantly from the concentrations achieved when employing targeted agents. ICG is injected in 0.2–0.5 mg/kg quantities, i.e., up to 25 mg systemically or ~1 mg for intratumoral administration. ICG video-angiography typically observes ICG before clearance, while it is still concentrated within the vascular system. With an average blood pool volume of 5 L in humans, 25 mg of intravenously administered ICG amounts to ~32 μmol or a concentration in the range of 0.6–6 μM assuming some clearance takes place during the measurement.

Targeted agents have been administered in amounts varying from 4.5 mg per patient to 62.5 mg/m^2 skin surface or ~150 mg per patient (55). However, fluorescence molecular imaging operates on the principle that the targeted agent clears from the vasculature and the surrounding tissue, so that only the agent with affinity to the biomarker selected is visualized. The agent concentrates in tumors or smaller volumes associated with remnant disease, infiltrating borders or small tumor foci. A very small percentage of the amount initially injected is available for detection. Assuming a loading ratio of three dye molecules per antibody (68), the amount of intravenously administered bevacizumab-800CW is approximately 30–300 nmol, assuming an injection of 4.5–45 mg, or 90–900 nmol of 800CW dye (ClinicalTrials.gov NCT01508572). Therefore, the amount of fluorochrome injected in these studies may be three orders of magnitude lower than in ICG video-angiography. Assuming only a small fraction of the agent targets disease, e.g., only 0.1–1% of the total administered dose reaches the tumor or infiltrates the border, the actual concentration at which fluorescence imaging of targeted agents works may be 5–6 orders of magnitude lower than the concentrations employed in ICG video-angiography. This characteristic of targeted dyes can be only partially compensated for by using dyes of higher quantum yield than ICG.

The different sensitivity requirements in detecting targeted versus nontargeted dyes delineate the more general issue of selecting the specifications of the imaging system clinically deployed. The sensitivity of a camera can play a critical role in the overall imaging quality and accuracy achieved. In addition to camera sensitivity, fluorescence images depend on multiple parameters, including the specifications of the optical system (lenses, endoscope), the illumination parameters (energy, wavelengths), and the dynamic range of the camera. Operation in hybrid mode, delivering registered white light and fluorescence images, or the capacity for multispectral measurements can further influence the nature of the data collected. In particular, operation in real-time mode may place strict requirements on the sensitivity and noise floor of a camera.

Today there are no established guidelines for fluorescence imaging; there exists great variability of camera technologies and performance. We expect that although hardware specifications will remain critical, software and algorithmic corrections will play an increasingly important role in delivering accurate fluorescence imaging solutions. It would therefore be important as a next step in the development of clinical fluorescence imaging to develop concepts that can impart standardization. For example, appropriate imaging targets can be developed that can be used as standards to evaluate key performance parameters, including sensitivity, camera cross-talk, and noise, in order to validate the imaging performance and allow studies to be compared to each other through a common reference.

CONCLUDING REMARKS

Greater precision in surgical intervention will require the use of advanced visualization methods that can pinpoint disease and differentiate it from sensitive healthy tissues. Human vision identifies surface tissue morphology but is not an ideal interventional guide, as it cannot visualize beneath

the surface of tissues and offers limited contrast. Visual navigation leaves the surgeon with no clear metrics during the procedure. Are the surgical margins free of cancer? Do the lymph nodes contain cancer?

Fluorescence imaging offers great potential for improved guidance. It is associated with optimizing surgical outcome and minimizing tissue damage and adverse postoperative side effects. Nevertheless, the capabilities of the method must be carefully considered for its successful implementation. Imaging of tissue perfusion using ICG offers a straightforward measurement, as long as the vasculature visualized is close to the surface, but conclusions regarding deeper tissues should be validated. Likewise, validation of the targeting ability of fluorescence agents should be performed using detection systems that offer appropriate accuracy and sensitivity to operate within the particular specifications of the dye selected. This is particularly important when using targeted agents at concentrations that may be markedly lower than those with ICG video-angiography. Surgical guidelines and training play an important role in adopting new technology and may explain the slow introduction of fluorescence imaging in the operating room despite its long history.

Current studies demonstrate a favorable outlook for fluorescence imaging and a growing interest in its mainstream clinical adoption. In addition, the increasing propagation of fluorescence imaging systems, especially as part of minimally invasive surgeries and robotic surgeries (69), will introduce more surgeons to the benefits of the modality. We expect in particular that minimally invasive surgery will be a major route of fluorescence imaging dissemination. Initial evidence indicates that fluorescence images will act as supplementary information to the conventional white light images, offering auxiliary guidance metrics. In our view, however, it is possible that in a few years, intraoperative guidance will be primarily based on the fluorescence signal, imparting certainty and precision, whereas color (white light) images will be employed only for anatomical orientation. This process is no different than similar developments in radiology, for example, combining X-ray computed tomography with positron emission tomography images (70, 71).

DISCLOSURE STATEMENT

V.N. has equity in SurgVision BV.

ACKNOWLEDGMENTS

The authors have received funding from the Deutsche Forschungsgemeinschaft (DFG), Germany (Leibniz Prize 2013; NT 3/10-1).

LITERATURE CITED

1. Roberts DW, Hartov A, Kennedy FE, et al. 1998. Intraoperative brain shift and deformation: a quantitative analysis of cortical displacement in 28 cases. *Neurosurgery* 43:749–58
2. Labadie RF, Davis BM, Fitzpatrick JM. 2005. Image-guided surgery: What is the accuracy? *Curr. Opin. Otolaryngol. Head Neck Surg.* 13:27–31
3. Zanzonico P, Heller S. 2000. The intraoperative gamma probe: basic principles and choices available. *Proc. Semin. Nucl. Med.* 30:33–48
4. Galloro G. 2012. High technology imaging in digestive endoscopy. *World J. Gastrointest. Endosc.* 4:22–27
5. Freschi C, Ferrari V, Melfi F, et al. 2013. Technical review of the da Vinci surgical telemanipulator. *Int. J. Med. Robot. Comput. Assist. Surg.* 9:396–406
6. Moore G, Hunter S, Hubbard T. 1949. Clinical and experimental studies of fluorescein dyes with special reference to their use for the diagnosis of central nervous system tumors. *Ann. Surg.* 130:637–42

7. Novotny H, Alvis D. 1960. A method of photographing fluorescence in circulating blood of the human eye. *Tech. Doc. Rep. SAM-TDR. USAF Sch. Aerosp. Med.* 60:1–4
8. Leevy CM, Smith F, Longueville J, et al. 1967. Indocyanine green clearance as a test for hepatic function: evaluation by dichromatic ear densitometry. *JAMA* 200:236–40
9. Rowell LB, Marx HJ, Bruce RA, et al. 1966. Reductions in cardiac output, central blood volume, and stroke volume with thermal stress in normal men during exercise. *J. Clin. Investig.* 45:1801–16
10. Craandijk A, Van Beek C. 1976. Indocyanine green fluorescence angiography of the choroid. *Br. J. Ophthalmol.* 60:377–85
11. Schaafsma BE, Mieog JSD, Hutteman M, et al. 2011. The clinical use of indocyanine green as a near-infrared fluorescent contrast agent for image-guided oncologic surgery. *J. Surg. Oncol.* 104:323–32
12. Polom K, Murawa D, Rho YS, et al. 2011. Current trends and emerging future of indocyanine green usage in surgery and oncology. *Cancer* 117:4812–22
13. Sekijima M, Tojimbara T, Sato S, et al. 2004. An intraoperative fluorescent imaging system in organ transplantation. *Transplant. Proc.* 36:2188–90
14. Holm C, Mayr M, Höfter E, et al. 2002. Intraoperative evaluation of skin-flap viability using laser-induced fluorescence of indocyanine green. *Br. J. Plastic Surg.* 55:635–44
15. Detter C, Russ D, Iffland A, et al. 2002. Near-infrared fluorescence coronary angiography: a new noninvasive technology for intraoperative graft patency control. *Proc. Heart Surg. Forum* 5:364–69
16. Ferroli P, Nakaji P, Acerbi F, et al. 2011. Indocyanine green (ICG) temporary clipping test to assess collateral circulation before venous sacrifice. *World Neurosurg.* 75:122–25
17. Allison AS, Bloor C, Faux W, et al. 2010. The angiographic anatomy of the small arteries and their collaterals in colorectal resections: some insights into anastomotic perfusion. *Ann. Surg.* 251:1092–97
18. Sherwinter DA. 2012. Transanal near-infrared imaging of colorectal anastomotic perfusion. *Surg. Laparosc. Endosc. Percutan. Tech.* 22:433–36
19. Jonsson K, Jensen JA, Goodson W 3rd, et al. 1991. Tissue oxygenation, anemia, and perfusion in relation to wound healing in surgical patients. *Ann. Surg.* 214:605–13
20. Yamaguchi S, De Lorenzi F, Petit JY, et al. 2004. The "perfusion map" of the unipedicled TRAM flap to reduce postoperative partial necrosis. *Ann. Plastic Surg.* 53:205–9
21. Azuma R, Morimoto Y, Masumoto K, et al. 2008. Detection of skin perforators by indocyanine green fluorescence nearly infrared angiography. *Plastic Reconstr. Surg.* 122:1062–67
22. Liu DZ, Mathes DW, Zenn MR, Neligan PC. 2011. The application of indocyanine green fluorescence angiography in plastic surgery. *J. Reconstr. Microsurg.* 27:355–64
23. Lyman GH, Temin S, Edge SB, et al. 2014. Sentinel lymph node biopsy for patients with early-stage breast cancer: American Society of Clinical Oncology clinical practice guideline update. *J. Clin. Oncol.* 32:1365–83
24. Yared M, Middleton L, Smith T, et al. 2002. Recommendations for sentinel lymph node processing in breast cancer. *Am. J. Surg. Pathol.* 26:377–82
25. Cox CE, Pendas S, Cox JM, et al. 1998. Guidelines for sentinel node biopsy and lymphatic mapping of patients with breast cancer. *Ann. Surg.* 227:645–53
26. Mieog JSD, Troyan SL, Hutteman M, et al. 2011. Toward optimization of imaging system and lymphatic tracer for near-infrared fluorescent sentinel lymph node mapping in breast cancer. *Ann. Surg. Oncol.* 18:2483–91
27. Wishart G, Loh S-W, Jones L, Benson J. 2012. A feasibility study (ICG-10) of indocyanine green (ICG) fluorescence mapping for sentinel lymph node detection in early breast cancer. *Eur. J. Surg. Oncol. (EJSO)* 38:651–56
28. Verbeek FP, Troyan SL, Mieog JSD, et al. 2014. Near-infrared fluorescence sentinel lymph node mapping in breast cancer: a multicenter experience. *Breast Cancer Res. Treat.* 143:333–42
29. Fujiwara M, Mizukami T, Suzuki A, Fukamizu H. 2009. Sentinel lymph node detection in skin cancer patients using real-time fluorescence navigation with indocyanine green: preliminary experience. *J. Plastic Reconstr. Aesthetic Surg.* 62:e373–e78
30. van den Berg NS, Brouwer OR, Klop WMC, et al. 2012. Concomitant radio- and fluorescence-guided sentinel lymph node biopsy in squamous cell carcinoma of the oral cavity using ICG-99mTc-nanocolloid. *Eur. J. Nucl. Med. Mol. Imaging* 39:1128–36

31. Crane L, Themelis G, Arts H, et al. 2011. Intraoperative near-infrared fluorescence imaging for sentinel lymph node detection in vulvar cancer: first clinical results. *Gynecol. Oncol.* 120:291–95
32. Crane LM, Themelis G, Pleijhuis RG, et al. 2011. Intraoperative multispectral fluorescence imaging for the detection of the sentinel lymph node in cervical cancer: a novel concept. *Mol. Imaging Biol.* 13:1043–49
33. Misiek M, Rzepka JK, Zalewski K, et al. 2014. Fluorescence-guided lymph node mapping with indocyanine green for endometrial cancer: a feasibility study. *Clin. J. Oncol.* (*Meet. Abstr.*) 32:e16549
34. Yamashita S-I, Tokuishi K, Miyawaki M, et al. 2012. Sentinel node navigation surgery by thoracoscopic fluorescence imaging system and molecular examination in non-small cell lung cancer. *Ann. Surg. Oncol.* 19:728–33
35. Rasmussen JC, Tan I-C, Marshall MV, et al. 2009. Lymphatic imaging in humans with near-infrared fluorescence. *Curr. Opin. Biotechnol.* 20:74–82
36. Abu-Rustum NR. 2014. Sentinel lymph node mapping for endometrial cancer: a modern approach to surgical staging. *J. Natl. Compr. Cancer Netw.* 12:288–97
37. Kim CH, Soslow RA, Park KJ, et al. 2013. Pathologic ultrastaging improves micrometastasis detection in sentinel lymph nodes during endometrial cancer staging. *Int. J. Gynecol. Cancer* 23:964–70
38. Marano A, Priora F, Lenti LM, et al. 2013. Application of fluorescence in robotic general surgery: review of the literature and state of the art. *World J. Surg.* 37:2800–11
39. Rossi EC, Ivanova A, Boggess JF. 2012. Robotically assisted fluorescence-guided lymph node mapping with ICG for gynecologic malignancies: a feasibility study. *Gynecol. Oncol.* 124:78–82
40. Jafari MD, Lee KH, Halabi WJ, et al. 2013. The use of indocyanine green fluorescence to assess anastomotic perfusion during robotic assisted laparoscopic rectal surgery. *Surg. Endosc.* 27:3003–8
41. Daskalaki D, Fernandes E, Wang X, et al. 2014. Indocyanine green (ICG) fluorescent cholangiography during robotic cholecystectomy: results of 184 consecutive cases in a single institution. *Surg. Innov.* 21:615–21
42. Frangioni JV. 2003. In vivo near-infrared fluorescence imaging. *Curr. Opin. Chem. Biol.* 7:626–34
43. van Oosten M, Crane LM, Bart J, et al. 2011. Selecting potential targetable biomarkers for imaging purposes in colorectal cancer using TArget Selection Criteria (TASC): a novel target identification tool. *Transl. Oncol.* 4:71–82
44. Moran MS, Schnitt SJ, Giuliano AE, et al. 2013. Society of Surgical Oncology–American Society for Radiation Oncology consensus guideline on margins for breast-conserving surgery with whole-breast irradiation in stages I and II invasive breast cancer. *Int. J. Radiat. Oncol. Biol. Phys.* 88:553–64
45. Fang W, Chen W, Chen G, Jiang Y. 2005. Surgical management of thymic epithelial tumors: a retrospective review of 204 cases. *Ann. Thorac. Surg.* 80:2002–7
46. Mendenhall WM, Zlotecki RA, Hochwald SN, et al. 2005. Retroperitoneal soft tissue sarcoma. *Cancer* 104:669–75
47. McCahill LE, Single RM, Aiello Bowles EJ, et al. 2012. Variability in reexcision following breast conservation surgery. *JAMA* 307:467–75
48. Tewari A, Sooriakumaran P, Bloch DA, et al. 2012. Positive surgical margin and perioperative complication rates of primary surgical treatments for prostate cancer: a systematic review and meta-analysis comparing retropubic, laparoscopic, and robotic prostatectomy. *Eur. Urol.* 62:1–15
49. Anderson C, Uman G, Pigazzi A. 2008. Oncologic outcomes of laparoscopic surgery for rectal cancer: a systematic review and meta-analysis of the literature. *Eur. J. Surg. Oncol.* 34:1135–42
50. van Dam GM, Themelis G, Crane LM, et al. 2011. Intraoperative tumor-specific fluorescence imaging in ovarian cancer by folate receptor-α targeting: first in-human results. *Nat. Med.* 17:1315–19
51. Hsiung P-L, Hardy J, Friedland S, et al. 2008. Detection of colonic dysplasia in vivo using a targeted heptapeptide and confocal microendoscopy. *Nat. Med.* 14:454–58
52. Atreya R, Neumann H, Neufert C, et al. 2014. In vivo imaging using fluorescent antibodies to tumor necrosis factor predicts therapeutic response in Crohn's disease. *Nat. Med.* 20:313–18
53. Sturm MB, Joshi BP, Lu S, et al. 2013. Targeted imaging of esophageal neoplasia with a fluorescently labeled peptide: first-in-human results. *Sci. Transl. Med.* 5:ra61
54. Scheuer W, van Dam GM, Dobosz M, et al. 2012. Drug-based optical agents: infiltrating clinics at lower risk. *Sci. Transl. Med.* 4:134ps11

55. Rosenthal EL, Warram JM, de Boer E, et al. 2015. Safety and tumor-specificity of cetuximab-IRDye800 for surgical navigation in head and neck cancer. *Clin. Cancer Res.* 21:3658–66
56. Stummer W, Novotny A, Stepp H, et al. 2000. Fluorescence-guided resection of glioblastoma multiforme utilizing 5-ALA-induced porphyrins: a prospective study in 52 consecutive patients. *J. Neurosurg.* 93:1003–13
57. Stummer W, Pichlmeier U, Meinel T, et al. 2006. Fluorescence-guided surgery with 5-aminolevulinic acid for resection of malignant glioma: a randomised controlled multicentre phase III trial. *Lancet Oncol.* 7:392–401
58. Kamp MA, Grosser P, Felsberg J, et al. 2012. 5-aminolevulinic acid (5-ALA)-induced fluorescence in intracerebral metastases: a retrospective study. *Acta Neurochir.* 154:223–28
59. Kishi K, Fujiwara Y, Yano M, et al. 2012. Staging laparoscopy using ALA-mediated photodynamic diagnosis improves the detection of peritoneal metastases in advanced gastric cancer. *J. Surg. Oncol.* 106:294–98
60. Harada K, Harada Y, Beika M, et al. 2013. Detection of lymph node metastases in human colorectal cancer by using 5-aminolevulinic acid-induced protoporphyrin IX fluorescence with spectral unmixing. *Int. J. Mol. Sci.* 14:23140–52
61. Riegger C, Herrmann J, Nagarajah J, et al. 2012. Whole-body FDG PET/CT is more accurate than conventional imaging for staging primary breast cancer patients. *Eur. J. Nucl. Med. Mol. Imaging* 39:852–63
62. Poulsen MH, Bouchelouche K, Høilund-Carlsen PF, et al. 2012. [18F] fluoromethylcholine (FCH) positron emission tomography/computed tomography (PET/CT) for lymph node staging of prostate cancer: a prospective study of 210 patients. *BJU Int.* 110:1666–71
63. Tichauer KM, Samkoe KS, Gunn JR, et al. 2014. Microscopic lymph node tumor burden quantified by macroscopic dual-tracer molecular imaging. *Nat. Med.* 20:1348–53
64. Nguyen QT, Tsien RY. 2013. Fluorescence-guided surgery with live molecular navigation—a new cutting edge. *Nat. Rev. Cancer* 13:653–62
65. Gibbs-Strauss SL, Nasr KA, Fish KM, et al. 2011. Nerve-highlighting fluorescent contrast agents for image-guided surgery. *Mol. Imaging* 10:91–101
66. Cotero VE, Siclovan T, Zhang R, et al. 2012. Intraoperative fluorescence imaging of peripheral and central nerves through a myelin-selective contrast agent. *Mol. Imaging Biol.* 14:708–17
67. Park MH, Hyun H, Ashitate Y, et al. 2014. Prototype nerve-specific near-infrared fluorophores. *Theranostics* 4:823–33
68. van Scheltinga AGT, van Dam GM, Nagengast WB, et al. 2011. Intraoperative near-infrared fluorescence tumor imaging with vascular endothelial growth factor and human epidermal growth factor receptor 2 targeting antibodies. *J. Nucl. Med.* 52:1778–85
69. Barbash GI, Glied SA. 2010. New technology and health care costs—the case of robot-assisted surgery. *N. Engl. J. Med.* 363:701–4
70. Gambhir SS. 2002. Molecular imaging of cancer with positron emission tomography. *Nat. Rev. Cancer* 2:683–93
71. Weber WA, Grosu AL, Czernin J. 2008. Technology insight: advances in molecular imaging and an appraisal of PET/CT scanning. *Nat. Clin. Pract. Oncol.* 5:160–70
72. Takami T, Yamagata T, Naito K, et al. 2013. Intraoperative assessment of spinal vascular flow in the surgery of spinal intramedullary tumors using indocyanine green videoangiography. *Surg. Neurol. Int.* 4:135
73. Buchs NC, Hagen ME, Pugin F, et al. 2012. Intra-operative fluorescent cholangiography using indocyanin green during robotic single site cholecystectomy. *Int. J. Med. Robot. Comput. Assist. Surg.* 8:436–40